NASA/TM—1998-206622

The Effect of Alloying on Topologically Close Packed Phase Instability in Advanced Nickel-Base Superalloy Rene N6

Frank Ritzert
Lewis Research Center, Cleveland, Ohio

David Arenas
Pennsylvania State University, State College, Pennsylvania

Dennis Keller
RealWorld Quality Systems, Inc., Rocky River, Ohio

Vijay Vasudevan
University of Cincinnati, Cincinnati, Ohio

Prepared for the
1998 Annual Meeting
sponsored by The Minerals, Metals, and Materials Society
San Antonio, Texas, February 15–19, 1998

National Aeronautics and
Space Administration

Lewis Research Center

May 1998

Trade names or manufacturers' names are used in this report for identification only. This usage does not constitute an official endorsement, either expressed or implied, by the National Aeronautics and Space Administration.

Available from

NASA Center for Aerospace Information
7121 Standard Drive
Hanover, MD 21076
Price Code: A03

National Technical Information Service
5287 Port Royal Road
Springfield, VA 22100
Price Code: A03

THE EFFECT OF ALLOYING ON TOPOLOGICALLY CLOSE PACKED PHASE INSTABILITY IN ADVANCED NICKEL-BASE SUPERALLOY RENE N6

Frank Ritzert
NASA Lewis Research Center
Cleveland, OH 44135

David Arenas
Penn State University
State College, PA 16801

Dennis Keller
RealWorld Quality Systems, Inc.
Rocky River, OH 44116

Vijay Vasudevan
Department of Materials Science and Engineering
University of Cincinnati
Cincinnati, OH 45221-0012

An investigation was conducted to describe topologically close packed (TCP) phase instability as a function of composition in the advanced Ni-base superalloy Rene N6. TCP phases are detrimental to overall high-temperature performance of Ni-base superalloys because of their brittle nature and because they deplete the Ni-rich matrix of potent solid solution strengthening elements. Thirty-four variations of polycrystalline Rene N6 determined from a design-of-experiments approach were cast and homogenized at 1315°C for 80 hours followed by exposure at 1093°C for 400 hours to promote TCP formation. The alloys had the following composition ranges in atomic percent: Co 10.61 to 16.73%, Mo 0.32 to 1.34%, W 1.85 to 2.52%, Re 1.80 to 2.11%, Ta 2.36 to 3.02%, Al 11.90 to 14.75%, and Cr 3.57 to 6.23%. Physical and chemical characteristics of all microstructures obtained were described using various analytical techniques. From these observations, a mathematical description of TCP occurrence (σ and P phase) was generated for polycrystalline Rene N6.

Introduction

Ni-base superalloy single crystals represent the state-of-the-art for turbine engine airfoil application as they offer the best balance of properties to allow for the high operating temperatures required for efficient engine operation.[1] Current trends in alloy design take advantage of improved creep rupture strength with the addition of higher levels of refractory elements.[2] In particular, the addition of significantly higher levels of Re in third generation superalloys is key for both microstructural stability and creep rupture strength.[3] While the presence of the refractories is thought to provide strength benefits from solid solution hardening, a tendency for alloy instability in the form of topologically-close-packed (TCP) phases or secondary reaction zone (SRZ) phenomena accompanies the high refractory content.[3] The formation of these phases in sufficient amount is detrimental to the overall high temperature performance of Ni-base superalloys because of their brittle nature and because they deplete the Ni-rich matrix of potent solid solution strengthening elements.[4] The tendency for a particular composition to form TCP may not be immediately known since the precipitation of TCP phases in Ni-base superalloys is nucleation controlled, thereby requiring long times at elevated temperatures to precipitate.[5] They preferentially nucleate along the octahedral planes of the Ni-base superalloys, usually in areas of refractory metal enrichment at grain boundaries or inside dendrites.[5,6] In Rene N6, two closely related TCP phases, σ and P, have been observed.[2]

Early attempts to predict TCP phase formation were based on the PHACOMP method,[7] which calculates an average electron vacancy number, N_v, for a given alloy. This theory is based on the premise that TCP phase precipitates in the γ phase when N_v of that γ phase exceeds a critical value.[8] The difficulty of PHACOMP was described by Murphy et. al.[9] who concluded that PHACOMP calculations are not accurate unless detailed knowledge is available as to the exact compositions of the precipitating phases. Efforts to predict TCP phase formation have continued into this decade by a group of Japanese authors who also make predictions based on the electronic structure of the Ni-base superalloy, commonly known as the "d-electrons method".[10,11] They have determined that 2 parameters, the bond order (Bo) and the average d-orbital energy level (Md) can be used to predict σ phase. As with the N_v method, the new method defines a critical value of Md above which instability occurs. This method also does not take into account the synergistic effects of the alloying elements on their partitioning behavior (i.e., the dependence of elemental partitioning on the presence or absence of other alloying elements).

Approach

The current work was designed to examine TCP phase formation in modern single crystal superalloys paying particular attention to the potential synergistic effects of alloying elements. In order to accomplish this, close attention must be paid to the structure and composition of all phases present. The approach chosen in this investigation to understand the presence of TCP phase instability in third generation Ni-base superalloys was to develop a model based on a design-of-experiments (DOE) methodology. While the investigation of multiple temperatures would have been of interest, it was instead decided to focus on one temperature and investigate the compositional effects in more detail. A DOE was set up to quantify both the linear and pairwise interactive effects of Al, Co, Cr, Mo, Re, Ta and W in an 8-component superalloy (Ni-base Rene N6 without C) on the resultant amount of TCP phase. It is a relative certainty that eventual turbine blade materials will be in single crystal form. However, to improve experimental feasibility and simplify the microstructures, it was decided to examine

the alloys in polycrystalline form and without the inclusion of carbon. The effects of those choices will be an increase in the likelihood of TCP in the microstructure due to the increased amount of high-energy grain boundary area and by precluding the formation of carbides. Although carbides may enhance TCP formation by providing more nucleation sites[12], the absence of carbon allows more refractory atoms that would be tied up in carbides to instead contribute to TCP. These choices are believed to be conservative in the sense that a single crystal is expected to have slightly less TCP formation than a polycrystal of the same composition. The full statistical model supported by the DOE was:

$$\begin{aligned}\text{TCP phase} = {} & \beta_0 + \beta_1X_1 + \beta_2X_2 + \beta_3X_3 + \beta_4X_4 + \beta_5X_5 + \beta_6X_6 + \beta_7X_7 + \\ & \beta_{12}X_1X_2 + \beta_{13}X_1X_3 + \beta_{14}X_1X_4 + \beta_{15}X_1X_5 + \beta_{16}X_1X_6 + \beta_{17}X_1X_7 + \\ & \beta_{23}X_2X_3 + \beta_{24}X_2X_4 + \beta_{25}X_2X_5 + \beta_{26}X_2X_6 + \beta_{27}X_2X_7 + \beta_{34}X_3X_4 + \\ & \beta_{35}X_3X_5 + \beta_{36}X_3X_6 + \beta_{37}X_3X_7 + \beta_{45}X_4X_5 + \beta_{46}X_4X_6 + \beta_{47}X_4X_7 + \\ & \beta_{56}X_5X_6 + \beta_{57}X_5X_7 + \beta_{67}X_6X_7 + [\beta_{81}B_1 + \beta_{82}B_2 + \beta_{83}B_3]\end{aligned}$$

where X_1=Al, X_2=Co, X_3=Cr, X_4=Mo, X_5=Re, X_6=Ta, X_7=W, β_o=intercept, and B_1, B_2, and B_3 are blocking terms. The ranges of investigation for each of the seven elements are listed in the next section. The 44 runs were conducted in four furnace batches of 11 experiments each. The DOE strategy employed is called D-Optimal.[13] This strategy allows the reliable estimation of a user-supplied model in the absolute minimum number of experiments. In this study the desired model incorporated 32 terms involving all seven linear effects of the alloying elements and 21 two-variable interactions that captured their interactive behaviors. The remaining 4 terms in the model were for the intercept and the three dummy variables that accounted for potential differences among the four furnace runs.

Material Selection

Rene N6 was chosen for this analysis because it is typical of third generation alloys.[14] Single crystal Rene N6 has a melting temperature of 1399°C and a γ' solvus of 1299°C.[15] A series of experimental superalloys with compositions containing Ni-Co-Al-Cr-Mo-W-Re-Ta were chosen based on Rene N6. In commercial Rene N6 trace amounts of C, B, and Hf are also present. Other elements not included in Rene N6, such as Ti and Y, may also contribute to phase instability in third generation Ni-base superalloys.

Forty-four Rene N6 compositions (thirty-four variations plus 10 repeats of one composition) were determined from a DOE strategy. The DOE defines a range of elements included at either their low or high limit as defined by the patent.[4] The alloys had the following composition ranges in atomic %: Co 10.61 to 16.73%, Mo 0.32 to 1.34%, W 1.85 to 2.52%, Re 1.80 to 2.11%, Ta 2.36 to 3.02%, Al 11.90 to 14.75%, and Cr 3.57 to 6.23%. The compositions studied are given in Table I. Alloys 1, 2, 3, 12, 13, 14, 23, 24, 25, 34, 35 were designed to be the repeats located at the middle composition level of each of the elements.

Procedure

All alloys were vacuum induction melted in argon starting with 100 gram charges of high-purity melting stock. The inductively stirred melts were then poured into a copper mold to obtain the cylindrical castings nominally 2 cm in diameter by 4 cm long. The heat treatment procedure was carried out in two steps. The goal of the first heat treatment was to fully homogenize the samples from top to bottom while the second heat treatment step would

Table I Compositions of all Rene N6 Castings in Atomic Percent With Actual and Predicted TCP Response

Alloy	Al	Co	Cr	Mo	Ni	Re	Ta	W	Vol % TCP	Predicted (vol%)
1	13.18	12.71	4.56	0.78	62.41	1.84	2.48	2.04	0.42	0.91±1.21
2	11.90	12.92	4.48	0.79	63.47	1.86	2.54	2.05	0.23	0.01±0.13
3	12.58	12.80	4.47	0.79	62.96	1.86	2.50	2.05	0.11	0.21±0.58
4	14.48	10.91	3.64	0.33	63.35	1.90	2.96	2.43	4.47	3.73±2.45
5	12.66	16.73	3.59	1.34	58.08	2.11	2.99	2.49	5.56	4.53±2.70
6	12.47	16.48	3.66	1.32	59.27	1.91	2.95	1.93	0.58	0.12±0.44
7	14.19	16.57	3.68	1.33	57.73	2.09	2.47	1.94	8.57	7.96±3.58
8	14.09	16.45	6.09	0.33	55.58	2.08	2.94	2.45	12.25	10.49±4.11
9	12.69	10.97	6.10	1.32	62.09	1.91	2.45	2.48	7.98	6.45±3.23
10	14.03	10.92	6.07	1.32	60.72	2.07	2.93	1.96	13.34	13.92±4.74
11	12.39	11.13	3.71	1.34	63.96	1.93	3.02	2.52	4.46	4.29±2.63
12	12.95	12.60	4.44	0.85	62.91	1.81	2.48	1.97	0.24	0.44±0.84
13	12.85	12.61	4.52	0.77	62.97	1.80	2.50	1.99	0.3	0.29±0.68
14	13.38	12.57	4.55	0.78	62.47	1.81	2.48	1.96	0.33	0.94±1.23
15	13.06	10.79	3.63	0.33	65.40	2.03	2.40	2.36	0.29	0.06±0.31
16	14.22	15.26	5.56	1.18	56.89	1.86	2.75	2.29	16.7	14.5±4.84
17	14.86	16.16	3.61	1.31	57.30	2.02	2.87	1.87	9.1	9.54±3.92
18	12.93	15.96	5.99	1.30	57.74	1.84	2.38	1.86	2.38	1.89±1.75
19	13.32	16.26	6.06	1.31	56.27	2.00	2.89	1.89	7.96	8.27±3.65
20	14.68	10.61	6.07	0.39	61.70	1.83	2.36	2.36	8.91	8.75±3.76
21	14.75	15.93	3.59	0.32	58.90	1.80	2.37	2.33	1.7	1.23±1.41
22	14.46	10.61	3.57	1.29	64.05	1.80	2.36	1.85	4.94	3.47±2.37
23	12.76	12.75	4.70	0.78	62.60	1.85	2.53	2.04	0.46	0.44±0.84
24	12.77	12.86	4.58	0.78	62.65	1.85	2.49	2.01	0.14	0.31±0.71
25	12.98	12.73	4.69	0.78	62.41	1.85	2.52	2.04	0.2	0.73±1.09
26	12.92	10.97	6.22	0.33	62.30	1.91	2.94	2.41	2.31	3.02±2.21
27	13.03	10.86	3.74	1.31	64.69	2.06	2.43	1.88	0.55	1.15±1.36
28	13.02	16.18	6.15	0.33	57.61	1.89	2.43	2.39	1.06	0.75±1.10
29	13.09	10.92	3.76	0.33	65.02	2.07	2.93	1.89	0.03	0.04±0.25
30	14.70	10.90	3.75	1.31	62.41	2.06	2.44	2.43	6.5	6.68±3.28
31	13.07	11.10	6.29	1.34	60.62	2.10	3.01	2.48	11	11.46±4.30
32	12.43	10.85	3.70	0.32	66.53	1.87	2.40	1.89	0	0.08±0.36
33	14.70	16.09	6.20	0.32	56.06	1.83	2.91	1.89	4.48	4.76±2.77
34	12.98	12.84	4.69	0.78	62.31	1.85	2.52	2.04	0.2	0.71±1.07
35	12.98	12.84	4.69	0.78	62.31	1.85	2.52	2.04	0.32	0.71±1.07
36	12.97	16.52	3.79	0.33	58.98	1.95	2.99	2.46	0.74	1.29±1.44
37	12.91	10.76	6.22	0.32	63.45	2.04	2.41	1.89	0.66	0.26±0.65
38	12.94	16.48	6.23	1.32	56.01	2.11	2.46	2.45	7.16	8.62±3.73
39	12.53	16.26	3.73	0.33	60.80	2.05	2.42	1.87	0	0±0
40	13.05	16.33	6.17	0.33	57.22	2.06	2.92	1.92	1.15	1.41±1.51
41	14.68	10.81	3.69	0.32	64.19	2.03	2.39	1.88	0.53	0.51±0.91
42	12.71	16.49	3.79	1.32	58.87	1.91	2.46	2.45	0.56	1.3±1.45
43	13.11	10.93	6.20	1.32	61.66	1.90	2.97	1.92	7.79	6.71±3.29
44	14.57	16.46	3.78	0.33	57.36	2.08	2.98	2.45	5.49	6.53±3.25

simulate the microstructural evolution of the alloys at unstressed, hot-engine conditions. Following a furnace calibration, all of the 44 alloys were homogenized in flowing argon at 1315°C for 80 hours. This was not a typical Rene N6 homogenization treatment. The longer time was chosen to minimize both macro and microsegregation in the castings. The homogenization procedure was carried out in four randomized batches of eleven samples each. All samples were air cooled from the homogenization treatment. Subsequent to homogenization, longer term heat treatments at 1093°C for 400 hours were conducted on all 44 as-homogenized samples using the same randomized array of four batches. The temperature 1093°C is considered to be a typical exposure for turbine blades in advanced engines.

Scanning electron microscopy was performed on all aged microstructures. Both secondary electron and backscatter electron imaging (BSE) were used to capture the predominantly three-phase ($\gamma+\gamma'+$TCP) aged microstructures. Since phase identification was important, BSE imaging was advantageous given the ability to capture compositional differences between phases in the form of intensity differences. Strong delineation of all microstructural phases allowed for more accurate quantitative image analysis.

Image analyses of the microstructures were performed using either a computerized image analysis software package or point counting as per ASTM Standard E562-95. The gray levels were set manually (by inspection) for each photograph when using the computer software. For each casting, four areas were analyzed and the results averaged.

Results

As-homogenized microstructures

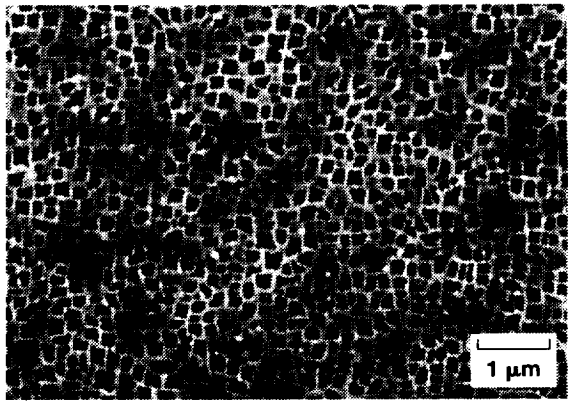

Figure 1 - As-homogenized microstructure.

The microstructural characteristics of the as-homogenized alloys were very diverse. Three as-homogenized alloys were strategically chosen for microprobe analyses to cover both lean and heavily alloyed compositions. The microprobe results indicated that no macro or microsegregation was present. Again, it is noted that carbides were absent in all alloys. Small amounts of TCP phase was observed in alloys 8, 10, 16, 30, and 31. The balance of the alloys exhibited the desired two-phase γ/γ' . γ' volume fractions ranged from 60 to 75 percent. The γ' precipitates were mostly cuboidal in shape (Figure 1) and ranged in size from 0.1 to 0.25 μm. Size differences could be the result of compositional variations, differences between

the homogenization temperature and the γ' solvus for each alloy, and slight differences in cooling rate from the homogenization treatment.

Aged microstructures

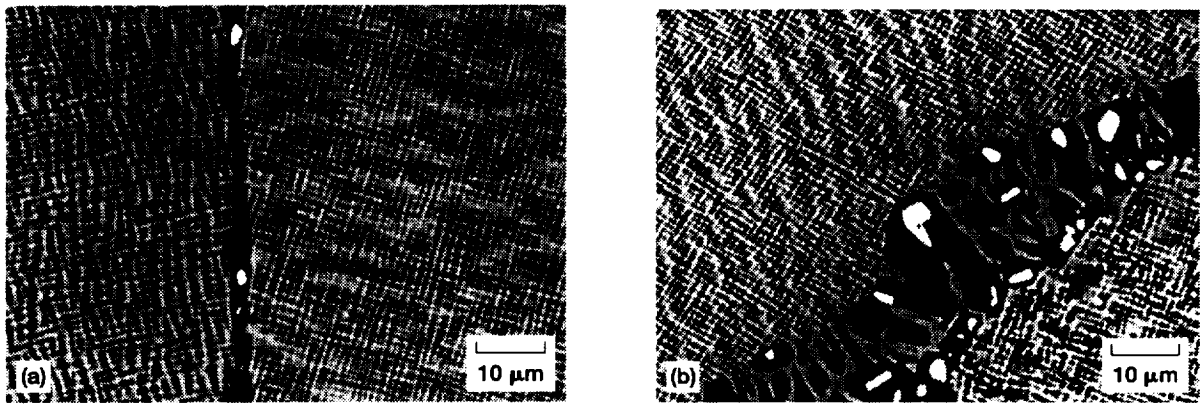

Figure 2 - Group 2 BSE images of aged microstructures indicating TCP only at grain boundaries. TCP is the white phase, γ is light gray, and γ' is dark gray. a) random formation, b) cellular formation.

Upon examination of all microstructures after aging treatment it was determined that the alloys fell into three groups based on the TCP distribution. Group 1 alloys contained no TCP phase and only alloys 32 and 39 were in this group. Group 2 was comprised of alloys where TCP formed exclusively at the grain boundaries and contained less than 3%TCP by volume. Further, Group 2 alloys could be broken down into two categories: 2a where the TCP existed as a random distribution along grain boundaries (Figure 2a) and 2b where the TCP tended to form in a cellular fashion (Figure 2b). Group 3 alloys contained between 3 and 17% TCP by volume. This third group was comprised of alloys that formed TCP at grain boundaries as well as within grains. Group 3 could be further broken down into three categories: isolated needles, interconnected needles, and abundant-random (Figures 3a-3c). Table II summarizes how all of the alloys were categorized.

Table II Breakdown of Alloy Microstructures into Groups

Group 1	Group 2		Group 3		
no TCP	Intergranular precipitates only		Intra- + inter-granular precipitation		
	random	cellular	isolated needles	interconnected needles	abundant/ random
32, 39	1,2,3,	6,21,26,	18,26,44	11,17,19,	4,5,7,
	12,13,14,	27,28,35,		22,38	8,9,10,
	15,23,24,	36,40,41,			16,17,19,
	25,26,28,	42			20,22,30,
	29,34,35,				31,33,38,
	36,37,42				43,44

The microstructures of the aged alloys were markedly different between Group 2 (Figure 2) and Group 3 (Figure 3) alloys. The γ/γ' structure within the grains of the Group 2 alloys was

undisturbed by the presence of TCP phase which was located at the grain boundaries. There was evidence of γ' alignment within the grains and also some evidence of γ' coarsening. Conversely, in regions near the TCP phase at the grain boundaries the γ' became the continuous phase at the expense of γ which is in agreement with the literature.[3] Group 2b alloys exhibited a cellular precipitation of phases at the grain boundaries including a variety of TCP phase morphologies while the TCP phase aspect ratio in Group 2a alloys was closer to 1. Group 3 alloys contained many different TCP phase morphologies. In all Group 3 alloys, the stable phase adjacent to the TCP phase was γ'. Group 3a contained a random placement of low TCP volume fraction while Group 3c formed TCP similarly but in more prolific amounts. Group 3b seemed to form TCP on preferred planes which are not conclusively identified at this time, however, {111} type planes are probable based on a measurement of roughly 54° from the {100} type γ' orientation. The TCP that was present in Group 3 alloys interrupted the γ/γ' structure but was most noticeable in the case of Group 3c where it is obvious that γ' was no longer present as discrete particles but as an interconnected, interpenetrating γ/γ' network.

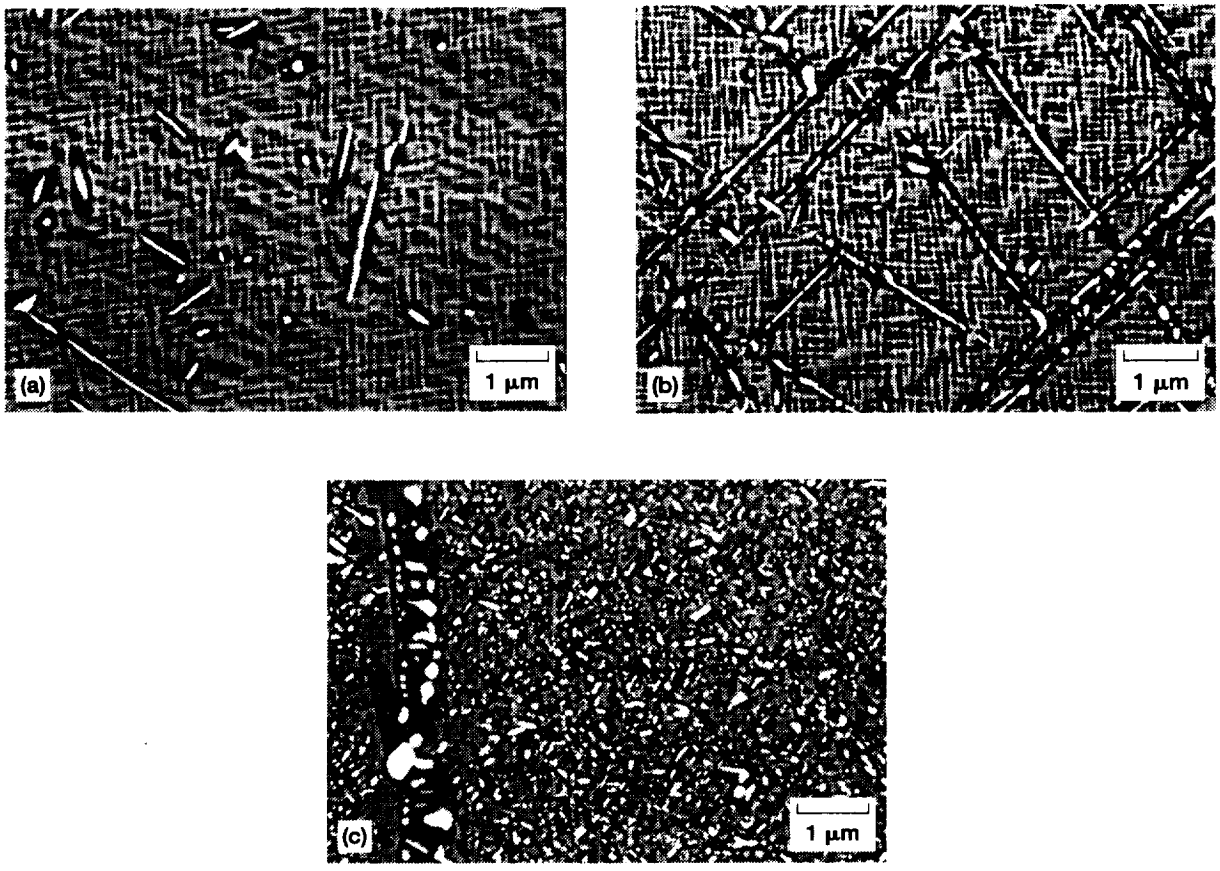

Figure 3 - Group 3 aged microstructures indicating both intra- and inter-granular TCP. a) isolated needles, b) interconnected needles, c) abundant/random.

Microprobe analyses of the TCP phase in a random sampling of 11 alloys indicated that it was rich in Re and Co. The average composition in atomic percent was: Ni 23.68, Co 19.60, Mo 5.40, W 12.30, Re 23.77, Ta 1.96, Al 0.44, and Cr 12.86. These values are meant to indicate the general trends in TCP phase composition because they represent a limited sampling and also because only the TCP at the grain boundaries was analyzed. As can be seen from Figures 2 and 3 it is obvious that the TCP phase cannot be classified as having any one

morphology. The TCP phase takes the form of needles, rods, and equiaxed particles depending on several factors, including composition and volume fraction. Transmission electron microscopy (TEM) in conjunction with electron diffraction conclusively identified both σ and P phases in the microstructure of alloy #17. The orthorhombic P-phase had lattice parameters of **a**=1.73nm, **b**=0.49nm, and **c**=0.92nm and the tetragonal σ phase had lattice parameters of **a**=0.931nm and **c**=0.486nm. It was not possible to distinguish σ from P using BSE contrast in the scanning electron microscope and TEM examination was not performed in sufficient detail to determine the relative amounts of the two phases. Therefore, the general designation of "TCP phase" is used to refer to the total volume fraction of σ plus P in all alloys.

Discussion

It is generally accepted that a complete understanding of the microstructure of complex Ni-base superalloys is elusive. While ternary and even quaternary systems can be described by phase diagrams, extrapolating those simpler cases for 8-component systems is often futile. It is of particular interest in this study to gain further understanding regarding the occurrence of TCP phase in third generation Ni-base superalloy microstructures. Future work will include analysis of compositional effects on the γ/γ' microstructure.

It is widely known that the refractory metal content in a Ni-base superalloy contributes to the formation of TCP phases such as σ and μ. This idea has also been substantiated by electron vacancy theory where the N_v values for the refractories are greater than N_v of other constituent elements. Most of the research substantiating this theory involved investigation of first- and second-generation Ni-base superalloys. Current Ni-base superalloys, termed third-generation, contained a greater amount of the refractory elements so as to improve the solid-solution strengthening of the alloy and improve its high-temperature engine performance. It is expected that the total refractory metal content in the alloys directly affects the TCP content. However, a strong sensitivity for both the type of refractory metal addition and also the level of other alloying elements exists. In other words, certain elements or combinations of alloying elements are more potent than others in forming TCP. It is situations such as these where DOE strategies are valuable as they employ multi-variable regression models to accurately quantify both the simple linear and complex interactive effects. A full multiple regression model is necessary in order to capture these effects.

Two approaches to model building were conducted in this work. The "backwards elimination with review" approach began with all 32 terms in the generic DOE model and sequentially eliminated the non-significant terms. The "forward selection with review" approach began with just an intercept and sequentially selected significant terms into the model. Both modeling approaches yielded the same final model. The actual regression calculations were performed on composition data that was in normalized units ranging from -1 to +1. Actual, not aim compositions were used. The volume percent of TCP was transformed by a square root function to accommodate the fact that TCP response values were more reproducible at lower volume % than they were at the higher volume fractions near 15%. Even though the blocking terms were significant, they were removed from the final model to make possible future predictions. The resultant decrease in agreement between actual and predicted TCP values was reflected in a slightly increased error of prediction. The result of this analysis in terms of atomic percent is:

$$(\text{vol\% TCP})^{1/2} = 16.344782 - 1.019587(\text{Al}) - 2.624322(\text{Cr}) - 3.821997(\text{Mo}) + 1.109575(\text{Re}) - 3.207295(\text{Ta}) + 6.462984(\text{W}) - 2.271803(\text{Co}) + 0.052884(\text{Al*Co}) + 0.214059(\text{Al*Cr}) + 0.300698(\text{Al*Mo}) + 0.80011(\text{Co*Re}) + 0.257108(\text{Cr*Mo}) - 5.081598(\text{Re*W}) + 1.824441(\text{Ta*W})$$

The model's predictive capability can be expressed by an approximate 95% confidence interval around the predicted value, and is given by TCP $\pm$ $1.27(\text{TCP})^{1/2}$. The model's goodness of fit is captured in the statistic $R^2 = 0.954$, which implies that 95.4% of the total variation in the response, $(\text{vol\% TCP})^{1/2}$, across all 44 experiments is explained by the model. Actual TCP volume percents as well as model predicted TCP phase values with 95% confidence intervals are given in Table I. Since the TCP prediction relies heavily on interactive effects as well as linear effects, its usefulness will be limited when applied to alloys that lie outside of the design space of Rene N6. The casting and heat treatment of several different alloys is forthcoming to experimentally verify the predictive capabilities of the model.

The above mathematical relationship indicates that every element in the composition can have a statistically significant effect on TCP phase formation. However, it is not simple to discern the direct relationship between the coefficients associated with individual elements and their primary effect on resultant TCP. In other words, coefficients associated with the linear effects of the elements can not be relied upon solely for indicating TCP phase response. Interactive effects captured by the interaction terms are also of critical importance, namely Co*Re, Mo*Cr, Cr*Al, Co*Al, Mo*Al, W*Re, and W*Ta. Figures 4a-4f represent these relationships graphically where volume % TCP phase is the response with uniform scaling across all graphs to indicate the relative strength of interactions. The response surface for Mo*Al was omitted because it was essentially identical to the Cr*Al response. For the generation of each graph, all 5 elements that were not included in the interactive relationship were kept at their midpoint compositional level. Figure 4a shows the response surface of volume percent TCP as a function of Re and Co content. The figure indicates that at low Co levels the inclusion of Re has very little effect on TCP content. However, when the Co level is high Re has a more pronounced, positive effect on TCP phase content. Figure 4b and 4c indicate that at higher levels of Cr, either high Mo or high Al levels contribute strongly to TCP formation. Conversely, the effect of Cr is negligible with low Al. Figure 4d shows that Co has less of an impact on TCP at lower Al levels and that the increase of Al across all Co levels contributes toward more TCP. Figures 4e and 4f show that the interactive effect of W with either Ta or Re gives a more subtle TCP response similar to that observed in the Co*Re interaction in Figure 4a. From inspection, the interactive effects of Re, W, and Ta are not major with respect to some of the other sharper trends toward high TCP content. The survey of Figures 4c-4e strongly suggests low Al levels to minimize TCP phase content. Figure 4b, when studied in conjunction with Figures 4c and 4e makes investigation of potential 3-way interaction among Mo, Cr, and Al intriguing for future studies. Further detailed inspection of the response surfaces in Figures 4a-4g could provide several additional, substantive arguments regarding the interactive effects of two elements on TCP.

If we were to look at this model using the Rene N6 target composition (Table III) a TCP content of 1.57 ± 1.59 percent after exposure to 1093°C for 400 hours is predicted. This is a

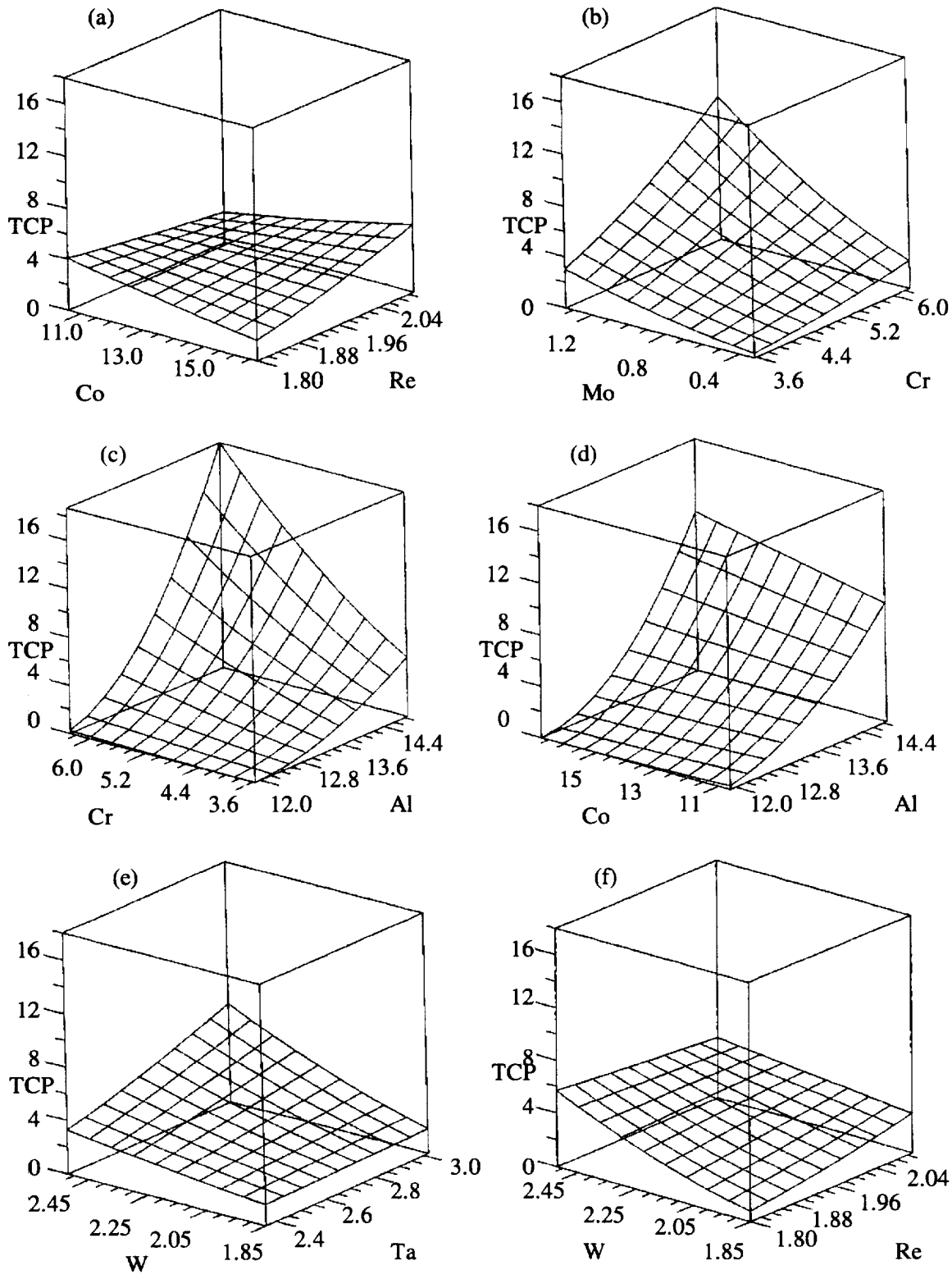

Figure 4 - Graphical representation of model predictions showing significant linear interactive effects. a)Co*Re, b)Mo*Cr, c)Al*Cr, d)Co*Al, e)W*Ta, f)W*Re.

reasonable result for Rene N6 close to its target composition. However, it is fair to assume from the results of this study that TCP content could become much higher if compositions of certain elements are at their high or low limits, but still within the specification of the alloy. Table III applies the mathematical description of TCP occurrence generated in this study to

several commercially available alloys. The trace elements present in the alloys were omitted from the table to simplify the application of the model while higher Ni values were used to absorb the excluded values and bring the compositions to 100 percent. Although Ti is not included in the model, it was assumed and treated to behave similar to Ta. In each case, the predicted TCP phase content is paired with a 95% confidence number. The obvious, inflated prediction of Rene N5 TCP content indicates that the "model" is not applicable to all second and third generation Ni-base superalloys. Especially those falling outside the design parameters of this study. By inspection it appears that the low Co level may be the main source for this discrepancy. The other predicted results of Table III appear believable after exposure at 1093°C for 400 hours.

Table III Compositions of Several Commercially Available Alloys in Atomic Percent

Alloy	W	Re	Ta	Cr	Mo	Al	Co	Ti	"Ni"	TCP
Rene N4	1.9	0	1.3	10.3	1.2	8.1	8.1	5.2	63.8	0
CMSX 4	2	1	2.2	7.6	0.4	12.6	9.3	1.3	63.8	7.55±3.49
Rene N5	1.6	1	2.3	8.1	1.3	13.9	8.2	0	63.6	23.09±6.10
Rene 162	1.9	2.1	2.4	5.4	0	14.3	13.1	0	60.8	1.53±/1.57
CMSX 10	1.7	2	2.8	2.4	0.3	13.2	3.2	0.3	74.2	0
Rene N6	2	1.8	2.5	5	0.9	13.3	13.2	0	61.2	1.57±1.59

CMSX-4® and CMSX-10® are registered trademarks of the Cannon-Muskegon Corporation.

Summary and Conclusions

An approach based on a DOE was conducted to describe TCP phase instability as a function of chemical content in advanced Ni-base superalloy Rene N6. A regression model was developed to describe the presence of TCP phase in the microstructures of polycrystalline Rene N6 based on chemical content. Forty-four alloys were cast, homogenized, and aged to produce samples for microstructural evaluations. For compositions all within the specification limits of the patent, TCP content varied from 0 to 17 volume percent. It was determined that Al, Mo, Cr, W, Re, and Ta had strong primary as well as interactive effects on the presence of TCP phase. While these primary effects can be described by PHACOMP, the present work was able to also quantify interaction effects which are difficult to obtain in PHACOMP-based approaches. For example, this study found the following interactions to be significant in varying degrees: Al*Co, Al*Cr, Al*Mo, Co*Re, Cr*Mo, Re*W, and Ta*W. The model was accurate (R^2=0.954) within the alloy design space, but extrapolation to other alloys is of unknown utility. The predictive capabilities of this model still require experimental verification but it did produce a reasonable prediction for a target composition of single crystal Rene N6.

References

1. Decker, R.F. and Sims, C.T. "The Metallurgy of Nickel-Base Alloys", The Superalloys, ed. Sims & Hagel, 1972, p.33.
2. Walston, W.S.; Schaeffer, J.C., Murphy, W.H., A New Type of Microstructural Instability in Superalloys - SRZ, Proceedings of Superalloys Symposium, Seven Springs, PA, September 22-26, 1996.

3. Walston, W.S.; O'Hara, K.S.; Pollock, T.M.; Murphy, W.H., Rene N6: Third Generation Single Crystal Superalloy, Proceedings of Superalloys Symposium, Seven Springs, PA, September 22-26, 1996.
4. Walston, W.S.; Ross, W; O'Hara, K.S.; Pollock, T.M., U.S. Patent Number 5,270,123, December 14, 1993.
5. Duhl, D.N. Alloy Phase Stability Requirements in Single Crystal Superalloys, Alloy Phase Stability and Design; Proceedings of Symposium, San Francisco, CA, April 18-20, 1990, p.389.
6. Sims, C.T., "Prediction of Phase Composition", Superalloys II, ed. Sims, Stoloff, & Hagel, 1987, p.217.
7. Woodyatt, L.R., Sims, C.T., and Beattie, H.J., Prediction of Sigma-Type Phase Occurrence from Compositions in Austenitic Superalloys, Trans. Met. Soc. AIME, Vol.236, April 1966, p.519.
8. Machlin, E.S. and Shao, J., SIGMA-SAFE: A Phase Diagram Approach to the Sigma Phase Problem in Ni Base Superalloys, Met. Trans. A, Vol.9A, April 1978, p.561.
9. Murphy, H.J.; Sims, C.T.; and Beltran, A.M., PHACOMP Revisited, Journal of Metals, November 1968, p.46.
10. Zhang, J.S.; Hu, Z.Q.; Murata, Y.; Morinaga, M.; and Yukawa, N., Design and Development of Hot Corrosion-Resistant Nickel-Base Single-Crystal Superalloys by the d-Electrons Alloy Design Theory: Part I. Characterization of the Phase Stability, Met Trans A, Vol.24A, November 1993, p.2443.
11. Yukawa, N.; Morinaga, M.; Murata, Y.; Ezaki, H.; and Inoue, S., High Performance Single Crystal Superalloys Developed by the d-Electrons Concept, in Superalloys 1988, p.225.
12. Sims, C.T., A Contemporary View of Nickel-Base Superalloys, Journal of Metals, October 1966, p.1119.
13. Bach, G.E.P., Draper, N.R., "Empirical Model-Building and Response Surfaces", Wiley Publishers, 1987, pp. 489-501.
14. Erickson, G.L., A New, Third-Generation, Single-Crystal, Casting Superalloy, Journal of Materials, April 1995.
15. Walston, W.S., personal communication.

REPORT DOCUMENTATION PAGE

Form Approved
OMB No. 0704-0188

1. AGENCY USE ONLY (*Leave blank*)	2. REPORT DATE	3. REPORT TYPE AND DATES COVERED
	May 1998	Technical Memorandum

4. TITLE AND SUBTITLE

The Effect of Alloying on Topologically Close Packed Phase Instability in Advanced Nickel-Base Superalloy Rene N6

5. FUNDING NUMBERS

WU-523-21-13-00

6. AUTHOR(S)

Frank Ritzert, David Arenas, Dennis Keller, and Vijay Vasudevan

7. PERFORMING ORGANIZATION NAME(S) AND ADDRESS(ES)

National Aeronautics and Space Administration
Lewis Research Center
Cleveland, Ohio 44135-3191

8. PERFORMING ORGANIZATION REPORT NUMBER

E-11058

9. SPONSORING/MONITORING AGENCY NAME(S) AND ADDRESS(ES)

National Aeronautics and Space Administration
Washington, DC 20546-0001

10. SPONSORING/MONITORING AGENCY REPORT NUMBER

NASA TM—1998-206622

11. SUPPLEMENTARY NOTES

Prepared for the 1998 Annual Meeting sponsored by The Minerals, Metals, and Materials Society, San Antonio, Texas, February 15–19, 1998. Frank Ritzert, NASA Lewis Research Center; David Arenas, Pennsylvania State University, State College, Pennsylvania 16801; Dennis Keller, RealWorld Quality Systems, Inc., Rocky River, Ohio 44116; Vijay Vasudevan, University of Cincinnati, Department of Materials Science and Engineering, Cincinnati, Ohio 45221-0012. Responsible person, Frank Ritzert, organization code 5120, (216) 433–8199.

12a. DISTRIBUTION/AVAILABILITY STATEMENT

Unclassified - Unlimited
Subject Category: 26 Distribution: Nonstandard

This publication is available from the NASA Center for AeroSpace Information, (301) 621–0390.

12b. DISTRIBUTION CODE

13. ABSTRACT (*Maximum 200 words*)

An investigation was conducted to describe topologically close packed (TCP) phase instability as a function of composition in the advanced Ni-base superalloy Rene N6. TCP phases are detrimental to overall high-temperature performance of Ni-base superalloys because of their brittle nature and because they deplete the Ni-rich matrix of potent solid solution strengthening elements. Thirty-four variations of polycrystalline Rene N6 determined from a design-of-experiments approach were cast and homogenized at 1315°C for 80 hours followed by exposure at 1093°C for 400 hours to promote TCP formation. The alloys had the following composition ranges in atomic percent: Co 10.61 to 16.73%, Mo 0.32 to 1.34%, W 1.85 to 2.52%, Re 1.80 to 2.11%, Ta 2.36 to 3.02%, Al 11.90 to 14.75%, and Cr 3.57 to 6.23%. Physical and chemical characteristics of all microstructures obtained were described using various analytical techniques. From these observations, a mathematical description of TCP occurrence (σ and P phase) was generated for polycrystalline Rene N6.

14. SUBJECT TERMS	15. NUMBER OF PAGES
Superalloy; Nickel; Instability	18
	16. PRICE CODE: A03

17. SECURITY CLASSIFICATION OF REPORT	18. SECURITY CLASSIFICATION OF THIS PAGE	19. SECURITY CLASSIFICATION OF ABSTRACT	20. LIMITATION OF ABSTRACT
Unclassified	Unclassified	Unclassified	